

Collective excitations in liquid bismuth

This article has been downloaded from IOPscience. Please scroll down to see the full text article.

2000 J. Phys.: Condens. Matter 12 3543

(<http://iopscience.iop.org/0953-8984/12/15/304>)

View [the table of contents for this issue](#), or go to the [journal homepage](#) for more

Download details:

IP Address: 171.66.16.221

The article was downloaded on 16/05/2010 at 04:48

Please note that [terms and conditions apply](#).

Collective excitations in liquid bismuth

Taras Bryk^{†‡} and Ihor Mryglod[†]

[†] Institute for Condensed Matter Physics, National Academy of Sciences of Ukraine,
1 Svientsitskii Street, UA-290011 Lviv, Ukraine

[‡] Department of Physics, University of Texas, Austin, TX 78712, USA

Received 1 November 1999, in final form 1 March 2000

Abstract. The spectrum of collective excitations of liquid-semimetal Bi is investigated within the generalized collective mode approach. From the analysis of spectra obtained for different basis sets of dynamical variables it is found that the high-frequency branch of propagating collective excitations corresponds to heat waves in the liquid. The contributions of different modes to density–density and energy–energy time correlation functions are discussed.

1. Introduction

Liquid metals are known as systems with well-defined collective excitations, which are visible in the dynamical structure factors $S(k, \omega)$ (k and ω being wavenumber and frequency, respectively) up to $k \sim 1 \text{ \AA}^{-1}$ [1]. For liquid semimetals and semiconductors the situation as regards manifestation of collective excitations in $S(k, \omega)$ is still not so clear as for metallic liquids and is under active study. For semimetallic Bi there was a report [2] on overdamped collective excitations, which were not found beyond $k \sim 0.6 \text{ \AA}^{-1}$ in $S(k, \omega)$ obtained by means of molecular dynamics (MD). Moreover, recently [3] the analysis of scattering experiments and molecular dynamics simulations of another semimetallic liquid, Ga, led to the conclusion of the existence of an additional ‘non-acoustic’ high-frequency branch in the spectrum of collective excitations.

Usually, the dynamics of binary systems has only been considered assuming the existence of several branches of propagating excitations. The high-frequency excitations in binary liquids were associated with the ‘fast-sound’ phenomenon [4–6] or with optic-like excitations in the case of ionic solutions [7, 8]. In the most recent investigation [9] it was shown that optic-like excitations exist even in mixtures of simple liquids and are caused by mass-concentration fluctuations. However, we have found only a few reports of investigations focused on the possibility of observing non-hydrodynamic excitations in simple liquids. In [10] the analysis of thermal neutron scattering experiments on liquid Cs and Rb near the melting point allowed the conclusion to be reached that the renormalization of the adiabatic sound velocity was caused by short-wavelength collective excitations called ‘zero-sound-like’ modes. However, neither in [10] nor in [3] was the origin of the non-acoustic collective excitations clearly established.

Only in the hydrodynamic limit ($k \rightarrow 0$, $\omega \rightarrow 0$) can the collective mode spectrum be studied analytically [11, 12]. For the longitudinal dynamics of pure liquids there exist three conserved variables: number density $\hat{n}(k, t)$, density of longitudinal current $\hat{J}_l(k, t)$, and energy density $\hat{e}(k, t)$. These three hydrodynamic variables correspond to three local conservation laws, which form a closed set of equations. The solution of the hydrodynamic

set of equations for pure liquids is well known: three eigenmodes determine the dynamics of pure liquid in the long-wavelength limit, namely the two sound waves propagating in opposite directions (a pair of complex-conjugate eigenvalues) and one relaxing thermodiffusive mode (a purely real eigenvalue).

Beyond the hydrodynamic region, short-time kinetic processes become very important and the standard hydrodynamics fails to explain the dynamics on a short-range scale. A generalized method was suggested in [13] for investigating the dynamical properties of a simple Lennard-Jones (LJ) liquid over a wide range of wavevectors. The main idea of this new method was an extension of the basis set of dynamical variables by including, in addition to the hydrodynamic ones, their time derivatives, which were supposed to describe short-time processes in liquids. The time evolution of these ‘extended’ variables was obtained in computer experiments carried out to evaluate the relevant time correlation functions and static averages. All static averages and some fitting parameters were used then to estimate the matrix elements of the secular equation derived from the generalized Langevin equation. In [14] this method of generalized collective modes (GCM) was modified into a parameter-free approach and in [15] was advanced to a high-number-of-variables approximation taking into account the first three time derivatives of the hydrodynamic variables in the basis set. In general, the basis set of N dynamical variables generated an $N \times N$ secular equation and resulted in N generalized collective modes (eigenvalues). The GCM method proved to be very useful for investigation of spectra of collective excitations in pure LJ liquids [13, 14], liquid-metallic Cs [16, 17], liquid water [18], the ‘fast-sound’ mixture He₆₅Ne₃₅ [19, 20], the glass-forming liquid-metallic alloy Mg₇₀Zn₃₀ [9, 21], and the metallic molten alloy Li₄Pb [23].

Among the N eigenvalues, the lowest ones (three modes in the case of pure liquids, and four for binary systems) always correspond to the hydrodynamic modes, which behave at $k \rightarrow 0$ as predicted by linear hydrodynamics. All other eigenvalues are called *kinetic* modes; these correspond to the processes with short timescales and cannot be obtained by the standard hydrodynamic treatment. Just kinetic modes are responsible for the ‘fast-sound’ phenomenon in binary liquids and optic-like excitations in many-component fluids. However, no attention has been paid to the possibility of observing kinetic modes in the time correlation functions (TCFs) of pure liquids. Even the origin of the kinetic modes for pure systems is not known *a priori*. Therefore, the theoretical study of possible eigenmodes in pure metals and semimetals is of great interest.

The goals of this study are:

- (i) to obtain the spectrum of collective excitations within the high-number-of-variables approximation of the parameter-free method of generalized collective modes;
- (ii) to estimate the origin of the branches in the spectrum of longitudinal collective modes of liquid-semimetal Bi ($n = 0.0289 \text{ \AA}^{-3}$, $T = 578 \text{ K}$); and
- (iii) to focus on the contributions of different modes to the time correlation functions.

The paper is organized as follows: in section 2 we briefly describe the method; the results for the spectrum of collective excitations and mode contributions to TCFs are reported in section 3, and conclusions are given in section 4.

2. Details of calculations

Within the nine-variable approximation [15] of the parameter-free GCM method, for the case of longitudinal dynamics in pure liquids the basis set of dynamical variables consists of the following operators:

$$\mathbf{A}^{(9)}(k, t) = \left\{ n(k, t), J_l(k, t), e(k, t), \dot{J}_l(k, t), \dot{e}(k, t), \ddot{J}_l(k, t), \ddot{e}(k, t), \dddot{J}_l(k, t), \dddot{e}(k, t) \right\} \quad (1)$$

where the dots denote the orders of the time derivatives of the relevant operators. The basis set of dynamical variables is applied to generate the eigenvalue problem from the generalized Langevin equation in the Markovian approximation [14, 15]:

$$[z\mathbf{I} + \mathbf{T}(k)]\tilde{\mathbf{F}}_M(k, z) = \mathbf{F}^0(k, t = 0) \tag{2}$$

where $\tilde{\mathbf{F}}_M$ denotes the Laplace-transformed matrix of TCFs, which can be calculated from (2) in the Markovian approximation; \mathbf{I} is the identity matrix, and $\mathbf{F}^0(k, t)$ is the matrix of TCFs. It was shown in [14] that the generalized hydrodynamic matrix $\mathbf{T}(k)$ can be written in the Markovian approximation as follows:

$$\mathbf{T}(k) = -i\Omega(k) + \tilde{\mathbf{M}}(k, 0) = \mathbf{F}^0(k, 0)\tilde{\mathbf{F}}^0{}^{-1}(k, 0) \tag{3}$$

where $i\Omega(k)$ and $\tilde{\mathbf{M}}$ are the frequency matrix and the matrix of memory functions, respectively.

The basis set (1) is used to generate the 9×9 eigenvalue problem for the matrix $\mathbf{T}(k)$:

$$\sum_{j=1}^9 T_{ij}(k)X_{j,\alpha} = z_\alpha(k)X_{i,\alpha} \quad \alpha = 1, \dots, 9 \tag{4}$$

where $X_{j,\alpha}$ is an eigenvector which corresponds to the eigenvalue z_α .

In our case the 9×9 Hermitian matrix of static correlation functions $\mathbf{F}^0(k, t = 0)$ has the form

$$\mathbf{F}^0(k) = \begin{bmatrix} f_{nn} & 0 & f_{ne} & -ikf_{JJ} & 0 & 0 & -kf_{je} & ikf_{jj} & 0 \\ 0 & f_{JJ} & 0 & 0 & -if_{je} & -f_{jj} & 0 & 0 & if_{j\dot{e}} \\ f_{ne} & 0 & f_{ee} & -if_{je} & 0 & 0 & -f_{\dot{e}\dot{e}} & if_{j\dot{e}} & 0 \\ ikf_{JJ} & 0 & if_{je} & f_{jj} & 0 & 0 & -if_{j\dot{e}} & -f_{j\ddot{j}} & 0 \\ 0 & if_{je} & 0 & 0 & f_{\dot{e}\dot{e}} & -if_{j\dot{e}} & 0 & 0 & -f_{\ddot{e}\ddot{e}} \\ 0 & f_{jj} & 0 & 0 & if_{j\dot{e}} & f_{jj} & 0 & 0 & -if_{j\ddot{e}} \\ -kf_{je} & 0 & -f_{\dot{e}\dot{e}} & if_{j\dot{e}} & 0 & 0 & f_{\ddot{e}\ddot{e}} & -if_{j\ddot{e}} & 0 \\ -ikf_{jj} & 0 & -if_{j\dot{e}} & -f_{jj} & 0 & 0 & if_{j\ddot{e}} & f_{j\ddot{j}} & 0 \\ 0 & -if_{j\dot{e}} & 0 & 0 & -f_{\ddot{e}\ddot{e}} & if_{j\ddot{e}} & 0 & 0 & f_{\ddot{e}\ddot{e}} \end{bmatrix} \tag{5}$$

Similarly, taking into account [13, 14] the properties of the time correlation functions, one obtains for $\tilde{\mathbf{F}}^0(k) = \tilde{\mathbf{F}}^0(k, z = 0)$

$$\tilde{\mathbf{F}}^0(k) = \begin{bmatrix} \tau_{nn}f_{nn} & \frac{i}{k}f_{nn} & \tau_{ne}f_{ne} & 0 & f_{ne} & -ikf_{JJ} & 0 & 0 & -kf_{je} \\ \frac{i}{k}f_{nn} & 0 & \frac{i}{k}f_{ne} & f_{JJ} & 0 & 0 & -if_{je} & -f_{jj} & 0 \\ \tau_{nn}f_{ne} & \frac{i}{k}f_{ne} & \tau_{ee}f_{ee} & 0 & f_{ee} & -if_{je} & 0 & 0 & -f_{\dot{e}\dot{e}} \\ 0 & -f_{JJ} & 0 & 0 & if_{je} & f_{jj} & 0 & 0 & -if_{j\dot{e}} \\ -f_{ne} & 0 & -f_{ee} & if_{je} & 0 & 0 & f_{\dot{e}\dot{e}} & -if_{j\dot{e}} & 0 \\ -ikf_{JJ} & 0 & -if_{je} & -f_{jj} & 0 & 0 & if_{j\dot{e}} & f_{j\ddot{j}} & 0 \\ 0 & -if_{je} & 0 & 0 & -f_{\dot{e}\dot{e}} & if_{j\dot{e}} & 0 & 0 & f_{\ddot{e}\ddot{e}} \\ 0 & f_{jj} & 0 & 0 & -if_{j\dot{e}} & -f_{jj} & 0 & 0 & if_{j\ddot{e}} \\ kf_{je} & 0 & f_{\dot{e}\dot{e}} & -if_{j\dot{e}} & 0 & 0 & -f_{\ddot{e}\ddot{e}} & if_{j\ddot{e}} & 0 \end{bmatrix} \tag{6}$$

where

$$\tau_{ij}(k) = \frac{1}{F_{ij}^0(k, t = 0)} \int_0^\infty F_{ij}^0(k, t) dt \tag{7}$$

are the hydrodynamic correlation times, which contain information about time-dependent properties of the system within the parameter-free GCM method.

Equation (2) has analytic solutions in terms of eigenvectors and eigenvalues of the matrix $\mathbf{T}(k)$, namely,

$$\tilde{F}_{ij}^M(k, z) = \sum_{\alpha=1}^N \frac{G_{ij}^{\alpha}(k)}{z + z_{\alpha}(k)} \quad (8)$$

where

$$G_{ij}^{\alpha}(k) = \sum_{l=1}^N X_{i\alpha} X_{\alpha l}^{-1} F_{lj}^0(k, 0) \quad (9)$$

are the weight coefficients describing the relevant contributions from the collective modes $z_{\alpha}(k)$. In the time representation the solutions (8) have the form

$$F_{ij}^M(k, t) = \sum_{\alpha=1}^N G_{ij}^{\alpha}(k) \exp\{-z_{\alpha}(k)t\}. \quad (10)$$

Thus, for the basis set (1) each Markovian approximant $F_{ij}^M(k, t)$ is expressed as a weighted sum of $N = 9$ terms and each of them is associated with the α th effective collective mode $z_{\alpha}(k)$. The following properties of TCFs in the Markovian approximation are very important from the point of view of sum rules:

$$\int_0^{\infty} \mathbf{F}_M(k, t) dt = \int_0^{\infty} \mathbf{F}^0(k, t) dt \quad (11)$$

$$\mathbf{F}_M(k, t=0) = \mathbf{F}^0(k, t=0). \quad (12)$$

Using these equations one can show [22] that the Markovian approximants $F_{ij}^M(k, t)$ reproduce exactly the frequency moments of the relevant MD-derived hydrodynamic TCFs up to the 2Sth order, inclusive, where S denotes the highest order of the time derivatives of the hydrodynamic variables included in the basis set. With the choice (1), the density–density time correlation function is exactly reproduced up to the eighth frequency moment, while for the energy–energy TCF the first seven frequency moments coincide with the actual ones.

To apply the GCM method in calculations of collective excitation spectra of a particular liquid, one has to continue the computer experiment and evaluate directly the matrix elements in equations (5) and (6). Liquid Bi with number density $n = 0.0289 \text{ \AA}^{-3}$ at average temperature 578 K was studied by means of MD simulations in the standard microcanonical ensemble using a system of 1000 particles interacting through the oscillating potential $\Phi_{ij}(r)$ at constant volume $V = L^3$. The smallest wavenumber achieved in the MD was $k_{\min} = 0.1928 \text{ \AA}^{-1}$. The time evolution of the hydrodynamic variables and their time derivatives was observed during the production run over 3×10^5 steps. The effective two-body potential $\Phi_{ij}(r)$ was taken in an analytical form from [24]. This potential was obtained in the cited work by fitting the calculated static structure factor of liquid Bi to the experimental one. We would like just to mention that this potential is much weaker than the two-body potential used in [16, 17] for investigation of the dynamical properties of liquid Cs within the GCM method. We will compare some results with ones obtained in the case of liquid Cs, but more detailed study of the role of the interatomic potential in the behaviour of generalized thermodynamic quantities and spectra of collective excitations of liquid metals and semimetals will be reported elsewhere.

The following scales of energy, length, and time are used below for reduction of the dimensional quantities: $\varepsilon = k_B T$, $\sigma = k_{\min}^{-1}$, $\tau = \sigma(m/\varepsilon)^{1/2} = 3.42 \text{ ps}$.

3. Results and discussion

The static correlation functions $f_{nn}(k)$, $f_{ne}(k)$, $f_{ee}(k)$, and $f_{je}(k)$, evaluated directly by means of MD, are shown in figure 1. The static structure factor $S(k)$ calculated as the Fourier transform of the pair correlation function (shown by crosses) is in very good agreement with the static correlation function $f_{nn}(k)$, which indicates reliability of the static averages directly evaluated from the MD. Since within Newtonian dynamics any operator of the basis set $\mathbf{A}^{(9)}(k, t)$ can be expressed in an analytical form via the positions and velocities of particles as well as via spatial derivatives of the interatomic potential (see [14]), one can evaluate directly in MD

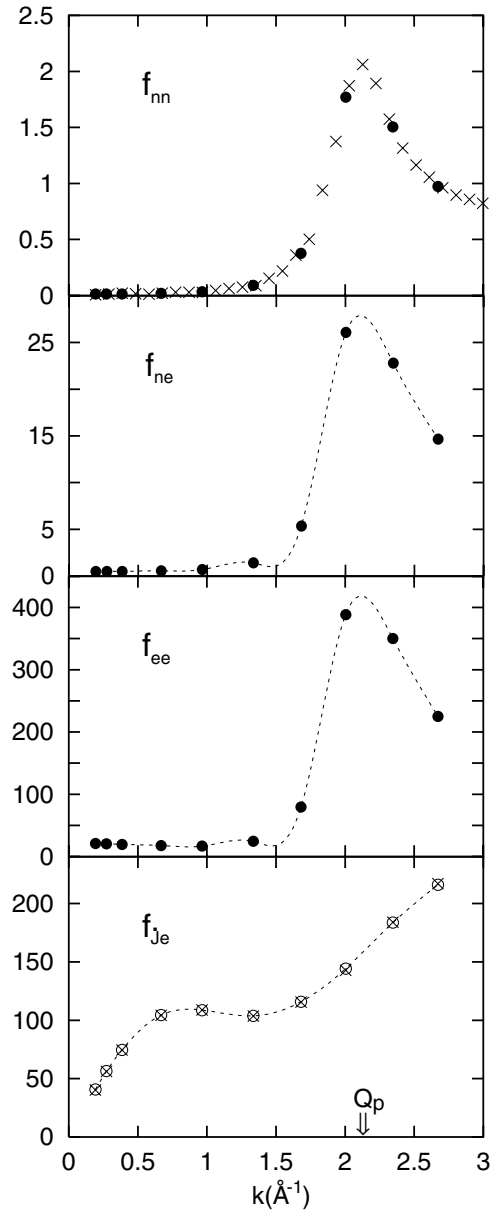


Figure 1. Static averages $f_{nn}(k)$, $f_{ne}(k)$, $f_{ee}(k)$, and $f_{je}(k)$, obtained directly in the MD (circles). Reduced units are used. The static structure factor $S(k)$, calculated as the Fourier transform of the radial distribution function, is shown by crosses in the top frame. In the bottom frame crosses correspond to the values of $f_{je}(k)$, obtained via numerical derivatives of the relevant time correlation function at $t = 0$. Dotted lines denote the spline interpolation. The double arrow denotes the position Q_p of the main peak of $S(k)$.

any static average for basis variables with the same precision. Having an analytical form of the interatomic potential, we have avoided the numerical evaluation of spatial derivatives of $\Phi_{ij}(r)$. This resulted in a very smooth k -dependence of the static averages evaluated directly in the MD. From figure 1 one can see that the static averages $f_{ne}(k)$ and $f_{ee}(k)$ have nearly the same features as the static structure factor (Q_p denotes the position of the main peak of $S(k)$), while $f_{je}(k)$ is a linear function of k when $k \rightarrow 0$. Another way of calculating $f_{je}(k)$ is via the numerical second-order time derivative of the time correlation function $F_{ne}(k, t)$ at $t = 0$. It is seen in figure 1 that the two methods (direct evaluation of static averages, shown by open circles, and via numerical second derivatives of relevant TCFs, shown by crosses) give almost identical values. In this study we used the second method of evaluation of static averages only for three static correlation functions involving operators with three dots. This allowed us to decrease substantially the duration of the MD production runs. All of the other static correlation functions were directly calculated in the MD.

Using our MD data for static correlation functions (shown in figure 1), we can also obtain the k -dependent generalized thermodynamic quantities [13, 14], namely,

$$H(k) = \frac{1}{k_B T k} f_{je}(k) \quad (13)$$

$$C_V(k) = \frac{1}{k_B T^2} [f_{ee}(k) - f_{ne}^2(k)/f_{nn}(k)] \quad (14)$$

$$\alpha(k)T = \frac{1}{k_B T} [H(k) f_{nn}(k) - f_{ne}(k)] \quad (15)$$

$$\gamma(k) = \frac{C_P(k)}{C_V(k)} \quad C_P(k) = C_V(k) + k_B T^2 \alpha^2(k)/f_{nn}(k) \quad (16)$$

where k_B denotes the Boltzmann constant, $H(k)$ is the generalized enthalpy per particle, $\alpha(k)$ is the generalized thermal linear expansion coefficient, and $C_V(k)$ and $C_P(k)$ are generalized specific heats at constant volume and constant pressure per particle, respectively. We show these generalized thermodynamic quantities in figure 2. There is a substantial difference in behaviour of the generalized thermodynamic quantities for liquid Bi in comparison with LJ fluid [14] and liquid-metallic Cs [16]. For example, the generalized enthalpy per particle does not change sign as a function of k as it did in the case for LJ liquid or Cs above the melting point. There is another interesting feature for the generalized linear expansion coefficient $\alpha(k)$. In the range $\sim(1.5-2.2) \text{ \AA}^{-1}$ this function of k takes negative values, while at $k \rightarrow 0$ it is close to the value of the linear expansion coefficient of solid Bi (shown by the asterisk at $k = 0$). The existence of a negative peak in $\alpha(k)$ is, perhaps, connected with the features of the interatomic potential and the relatively small kinetic energy of heavy particles of Bi. This conclusion is supported by the similar behaviour of $\alpha(k)$ in the case of Pb above the melting point [25], while at high temperatures this function for Pb is a positive function with a peak at Q_p , as was also obtained for liquid Cs [16]. The generalized specific heat at constant volume $C_V(k)$ has a maximum in the region of the main peak Q_p . The asterisk at $k = 0$ indicates the value of C_V obtained from the formulae for temperature fluctuations during the MD run. The generalized ratio of specific heats $\gamma(k)$ at $k \rightarrow 0$ is close to the value of γ for Bi at the melting point [1]. This function has a minimum at $k \sim 1.4 \text{ \AA}^{-1}$ with a value of ~ 1.0 , which indicates the region of applicability of viscoelastic theory for liquid Bi.

For the case of a simple liquid there exist three correlation times, which contain within the method of GCM all the information about time-dependent properties of the system investigated. In figure 3 we show the correlation times $\tau_{nn}(k)$, $\tau_{ne}(k)$, and $\tau_{ee}(k)$ multiplied by k^2 . One can see that the three functions are very similar and reflect the behaviour of the structure factor

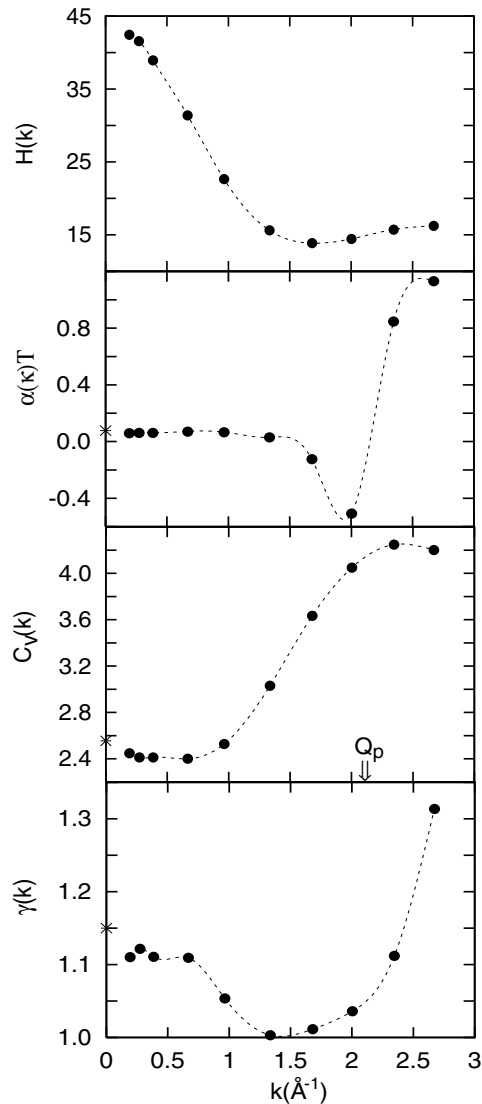


Figure 2. Generalized thermodynamic quantities for liquid Bi at 578 K (in reduced units): the generalized enthalpy per particle $H(k)$; the generalized linear expansion coefficient $\alpha(k)$; the generalized specific heat at constant volume per particle $C_V(k)$; the generalized ratio of specific heats $\gamma(k)$. Asterisks at $k = 0$ denote: $\alpha(k)T$ evaluated from the value known for solid Bi; for $C_V(k)$, the value obtained via temperature fluctuations in the MD; for $\gamma(k)$, the value at the melting temperature of Bi. Dotted lines denote the spline interpolation.

$S(k)$ over the entire k -range studied. At $k \rightarrow 0$ these correlation times, multiplied by k^2 , tend to non-zero values. The similarity of the three functions can be understood from figure 4, where the normalized density–density, density–energy, and energy–energy TCFs are shown for two wavenumbers. These functions display for small k -values strong oscillations with almost the same period. In contrast to the case for liquid Cs [16], where oscillations of energy–energy TCFs are overdamped even for small k -values, in liquid Bi the energy–energy and energy–density time correlation functions have even more pronounced oscillations than the

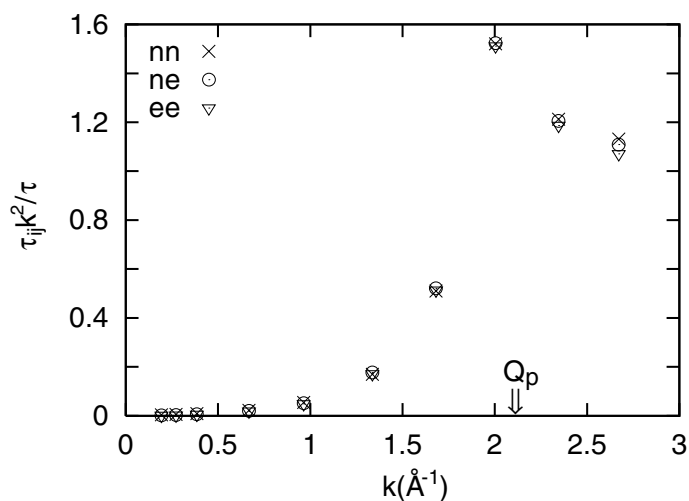


Figure 3. Correlation times $\tau_{nn}(k)$ (crosses), $\tau_{ne}(k)$ (open circles), and $\tau_{ee}(k)$ (open triangles), multiplied by k^2 , calculated from equation (7) on the basis of MD time correlation functions.

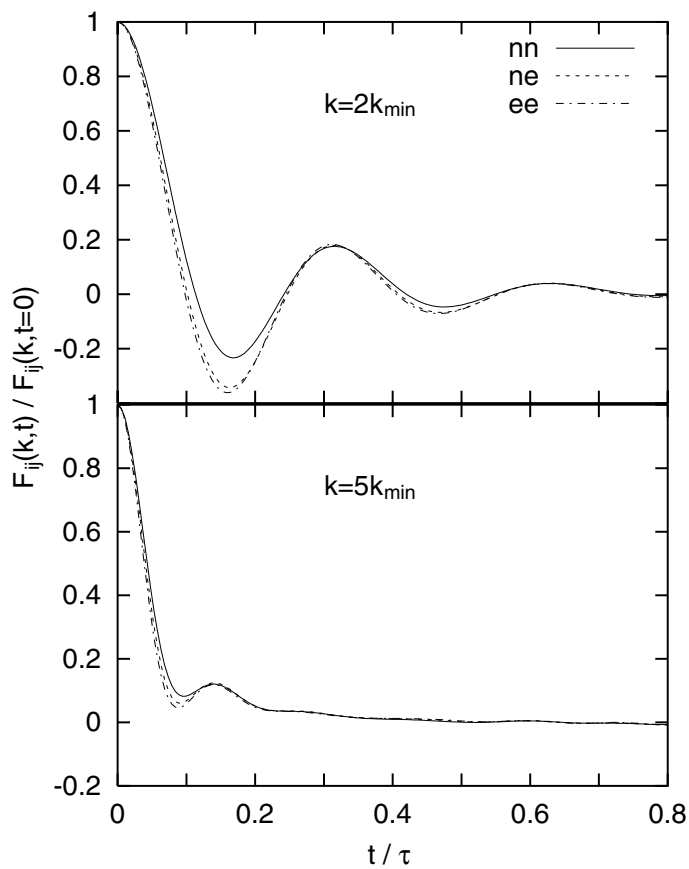


Figure 4. Normalized time correlation functions for two k -values: $F_{nn}(k, t)$ (solid line), $F_{ne}(k, t)$ (dashed line), $F_{ee}(k, t)$ (dashed-dotted line). k_{\min} and τ are 0.1928 \AA^{-1} and 3.42 ps , respectively.

density–density ones. Such a behaviour is observed in the k -region up to $\sim 1 \text{ \AA}^{-1}$.

The eigenvalues of the matrix $\mathbf{T}(k)$ for liquid Bi, obtained from the 9×9 secular equation (4) generated from the basis set (1), are shown in figure 5. As functions of k they form the spectrum of collective excitations. It is seen in figure 5 that the spectrum consists of three branches of propagating modes with complex eigenvalues:

$$z_{\alpha}^{\pm}(k) = \pm i\omega_{\alpha}(k) + \sigma_{\alpha}(k) \quad \alpha = 1, \dots, 3$$

and three purely real relaxing modes

$$\text{Im}\{z_{\alpha}^R(k)\} = 0 \quad \alpha = 1, \dots, 3.$$

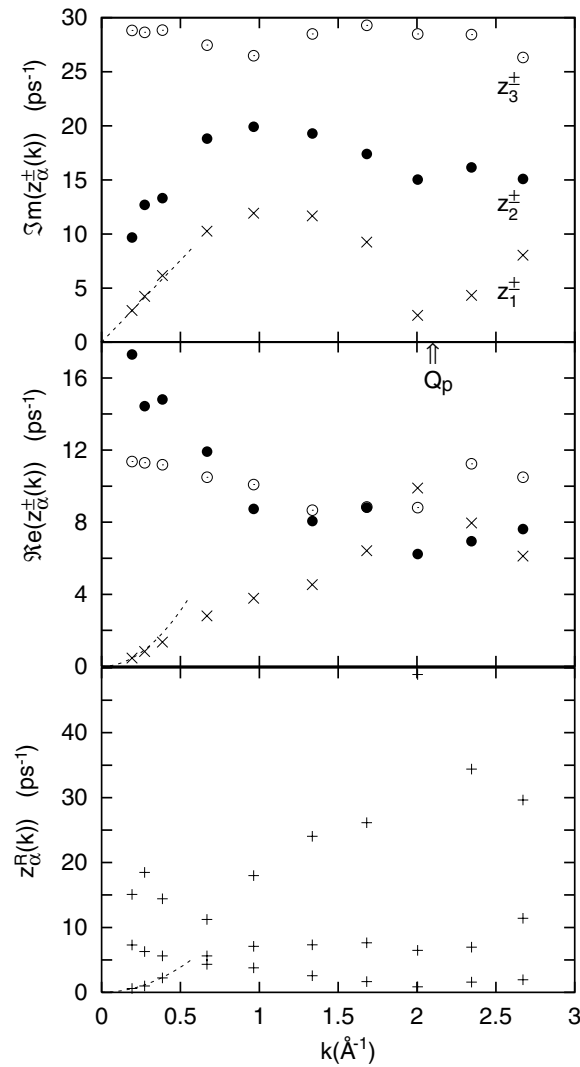


Figure 5. The spectrum of collective excitations of liquid Bi at 578 K, obtained for the nine-variable basis set $\mathbf{A}^{(9)}(k, t)$. Complex and purely real eigenvalues are shown by the symbols \times and $+$, respectively. The asymptotic hydrodynamic behaviour of the lowest eigenvalues is shown by dashed lines.

The imaginary parts of the eigenvalues in the case of liquid Bi are well separated, which allows one to easily distinguish different branches of propagating excitations $z_\alpha^\pm(k)$. However, this is difficult to perform for relaxing modes with purely real eigenvalues (the bottom frame in figure 5), because they are very close in the spectrum.

From the behaviour of the eigenvalues at $k \rightarrow 0$ one can estimate that the lowest pair of propagating modes $z_1^\pm(k)$ corresponds to the generalized acoustic excitations with linear dispersion $\omega_s(k)$:

$$z_1^\pm(k) \rightarrow \pm ic_s k + \Gamma k^2 \quad k \rightarrow 0. \quad (17)$$

The straight dashed line in the top frame of figure 5 makes it possible to see that the lowest branch $z_1^\pm(k)$ has a small ‘positive dispersion’ that is in complete agreement with predictions of mode-coupling analysis [26–28]. From the slope of this line we estimated the speed of longitudinal sound in liquid Bi to be $c_s = 1508.7 \text{ m s}^{-1}$, which is in perfect agreement with the experimental value of 1520 m s^{-1} [29, 30]. The real parts of $z_1^\pm(k)$, which determine the damping (or inverse lifetime) of the generalized sound excitations, in the hydrodynamic limit are functions of k^2 with the sound attenuation coefficient Γ . We estimated Γ to be $1.20 \times 10^{-7} \text{ m}^2 \text{ s}^{-1}$. Beyond the hydrodynamic region the mode-coupling effects become important and they change the dependence (17). For the case of the real parts of the eigenvalues $z_1^\pm(k)$, the departure from the hydrodynamic parabolic form (shown by the dashed line) displays negative dispersion; this is, again, in agreement with the predictions of mode-coupling analysis [26–28].

Another hydrodynamic eigenvalue, which is a purely real one and corresponds to the thermodiffusive mode, according to the predictions of hydrodynamics, behaves in the small- k region like

$$z_1^R(k) \rightarrow D_T k^2 \quad k \rightarrow 0 \quad (18)$$

with D_T being the thermodiffusion coefficient. From the smallest- k point we estimated the value $D_T = 1.546 \times 10^{-7} \text{ m}^2 \text{ s}^{-1}$. The dashed line with the dependence (18) almost coincides with the lowest purely real eigenvalue for the three smallest k -values. For this eigenvalue $z_1^R(k)$, however, there also exists a small negative departure from the form (18) beyond the hydrodynamic region due to mode-coupling effects.

A note should be added here about mode-coupling effects. We mean here the dynamical coupling between different collective modes, which results in shifts of the eigenvalues in comparison with ‘bare’ collective modes. The latter could be obtained within the relevant separated-variable treatment. These mode-coupling effects can be called ‘local’ ones since they take into account coupling of different modes with the same k -value only. One should distinguish these effects from the results of mode-coupling theory (see, e.g., [11, 31, 32]), in which non-local coupling of hydrodynamic modes for small k and ω is considered.

The pair of propagating modes $z_1^\pm(k)$ and the thermodiffusive mode $z_1^R(k)$ form the set of generalized hydrodynamic collective excitations. All other eigenvalues correspond to kinetic modes, which in the small- k limit, in contrast to generalized hydrodynamic ones, have finite damping coefficients (lifetime) and do not contribute to the long-wavelength dynamics. However, beyond the hydrodynamic region the real parts of the generalized hydrodynamic and kinetic modes can have comparable values.

Two high-frequency branches of kinetic propagating modes $z_2^\pm(k)$ and $z_3^\pm(k)$ have different dispersions. While the former has some features of the sound branch (a minimum in the region of Q_p , and a maximum at $\sim Q_p/2$), the latter is rather narrow. To find the origin of the high-frequency kinetic branches in the spectrum of collective excitations of liquid Bi, we proceed in the following way: (i) introduce orthogonal dynamical variables; (ii) calculate spectra of generalized modes from separated basis subsets generated by orthogonal dynamical

variables; (iii) compare spectra obtained from separated subsets and $\mathbf{A}^{(9)}$. In the case of weak mode-coupling effects, one can expect some branches of the spectrum obtained for the ‘coupled’ basis set $\mathbf{A}^{(9)}$ to be reproduced by branches obtained from separated subsets. A similar analysis performed for transverse spectra of binary liquids enabled us to find the optic-like excitations in non-ionic binary liquids [9].

We define the operator $\hat{h}(k, t)$:

$$\hat{h}(k, t) = \hat{e}(k, t) - \frac{f_{ne}}{f_{nn}} \hat{n}(k, t). \quad (19)$$

It is easily to verify that the operator $\hat{h}(k, t)$ is orthogonal to the density operator $\hat{n}(k, t)$, in contrast to the energy-density one. Now, the set of three variables $\hat{n}(k, t)$, $\hat{J}(k, t)$, $\hat{h}(k, t)$ contains only orthogonal variables and can be extended by including their time derivatives. The dynamical variable $\hat{h}(k, t)$ describes, in fact, the heat-density fluctuations [33, 34], and in the limit $k \rightarrow 0$ the thermodiffusive mode emerges exclusively due to heat-density fluctuations. In figure 6 the set of TCFs $F_{hh}(k, t)$ for different k -values is shown. One can see that even for k_{\min} this time correlation function does not have the single-exponential form, which is a result of coupling between heat and viscous processes [33].

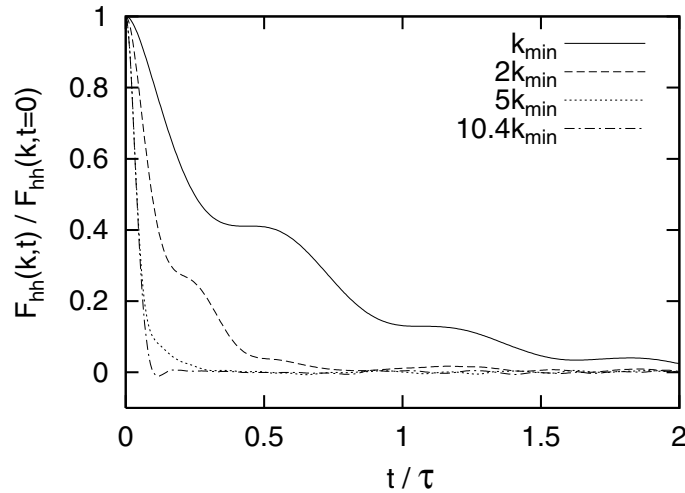


Figure 6. Normalized ‘heat-density–heat-density’ time correlation functions $F_{hh}(k, t)$ for four k -values. k_{\min} and τ are 0.1928 \AA^{-1} and 3.42 ps , respectively.

To understand the shape of the TCFs $F_{hh}(k, t)$ shown in figure 6, we generated a set of four dynamical variables:

$$\mathbf{A}^{(4h)}(k, t) = \left\{ h(k, t), \dot{h}(k, t), \ddot{h}(k, t), \dddot{h}(k, t) \right\}. \quad (20)$$

Another separated subset which can be considered does not contain a heat-density (or energy-density) operator or its time derivatives and consists of five operators:

$$\mathbf{A}^{(5)}(k, t) = \left\{ n(k, t), J_l(k, t), \dot{J}_l(k, t), \ddot{J}_l(k, t), \dddot{J}_l(k, t) \right\}. \quad (21)$$

The two subsets (20) and (21) form together a nine-variable basis, which can be obtained from $\mathbf{A}^{(9)}(k, t)$, equation (1), by linear transformation of variables. Hence, one can expect spectra of collective modes obtained from separated subsets (20) and (21) to give additional information about the origin of branches of the spectrum calculated from the ‘coupled’ nine-variable basis

set (1). In figure 7 the spectra of eigenvalues for the separated sets (20) and (21) are shown by closed and open boxes, respectively. It is seen that the second branch of propagating modes $z_2^\pm(k)$, as well as the lowest purely real eigenvalues $z_1^R(k)$, appear due to the heat-density fluctuations in the liquid. Thus, along with thermodiffusion there exist propagating heat modes (high-frequency heat waves) in liquid Bi. The third high-frequency branch of propagating modes $z_3^\pm(k)$ is derived from density fluctuations and, due to very high damping ($\text{Re}(z_3^\pm(k)) \sim 30 \text{ ps}^{-1}$), does not contribute significantly to the dynamical properties of the liquid. These excitations have extremely short lifetimes, which are defined as the inverses of the real parts of their eigenvalues.

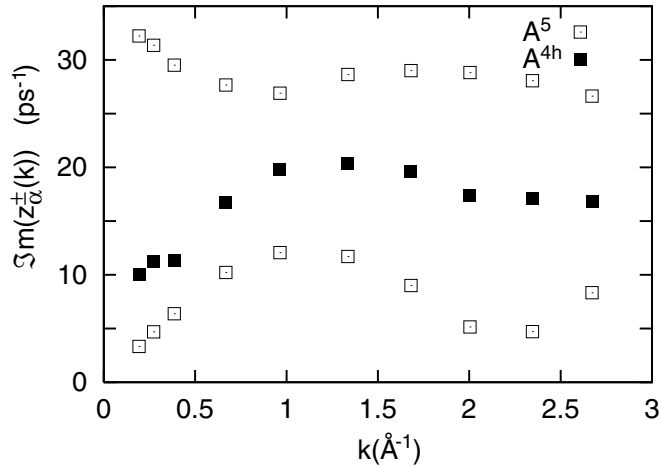


Figure 7. Spectra of propagating collective excitations, obtained for the separated subsets $\mathbf{A}^{(5)}(k, t)$ (shown by open boxes) and $\mathbf{A}^{(4h)}(k, t)$ (closed boxes).

The method of GCM makes it possible to investigate the separated mode contributions to various TCFs and the dynamic structure factor according to (10) and (8), respectively. We are interested mainly in the contributions of heat waves to the density–density time correlation functions, which appear due to the mode-coupling effects. In figure 8 we show by different lines the contributions of generalized hydrodynamic modes (acoustic $z_1^\pm(k)$ and thermodiffusive $z_1^R(k)$) and kinetic heat modes $z_2^\pm(k)$ to density–density TCFs. It is seen that within the nine-variable approximation of the GCM method the solutions for time correlation functions (10), shown by solid lines, reproduce very nicely MD-derived time correlation functions (diamond symbols). For the smallest wavevector k_{\min} , the shape of $F_{nn}(k, t)$ is mainly defined by acoustic modes. On increasing k the contribution of the branch z_1^\pm decreases, while that of the mode $z_1^R(k)$ increases, and for $k \sim Q_p$ becomes dominant. One can see that in the case of liquid Bi the heat waves (kinetic collective propagating modes $z_2^\pm(k)$) have almost zero weight for all k -values investigated. Their contributions are two orders of magnitude smaller than the ones from the three hydrodynamic modes: acoustic excitations and the thermodiffusive mode.

The contributions of heat waves, however, can be seen in the ‘heat-density–heat-density’ time correlation function. In figure 9 the function $F_{hh}(k, t)$ as well as the separated mode contributions are shown for two k -values. Interestingly, the oscillations of this time correlation function for $k = k_{\min}$ are caused by acoustic excitations, although the dominant contribution is from the thermodiffusive purely real mode $z_1^R(k)$. This result is obvious, because the real parts of sound modes are much smaller than those of heat waves in the small- k region, and this produces the big difference in their contributions. However, for larger k -values the weights of

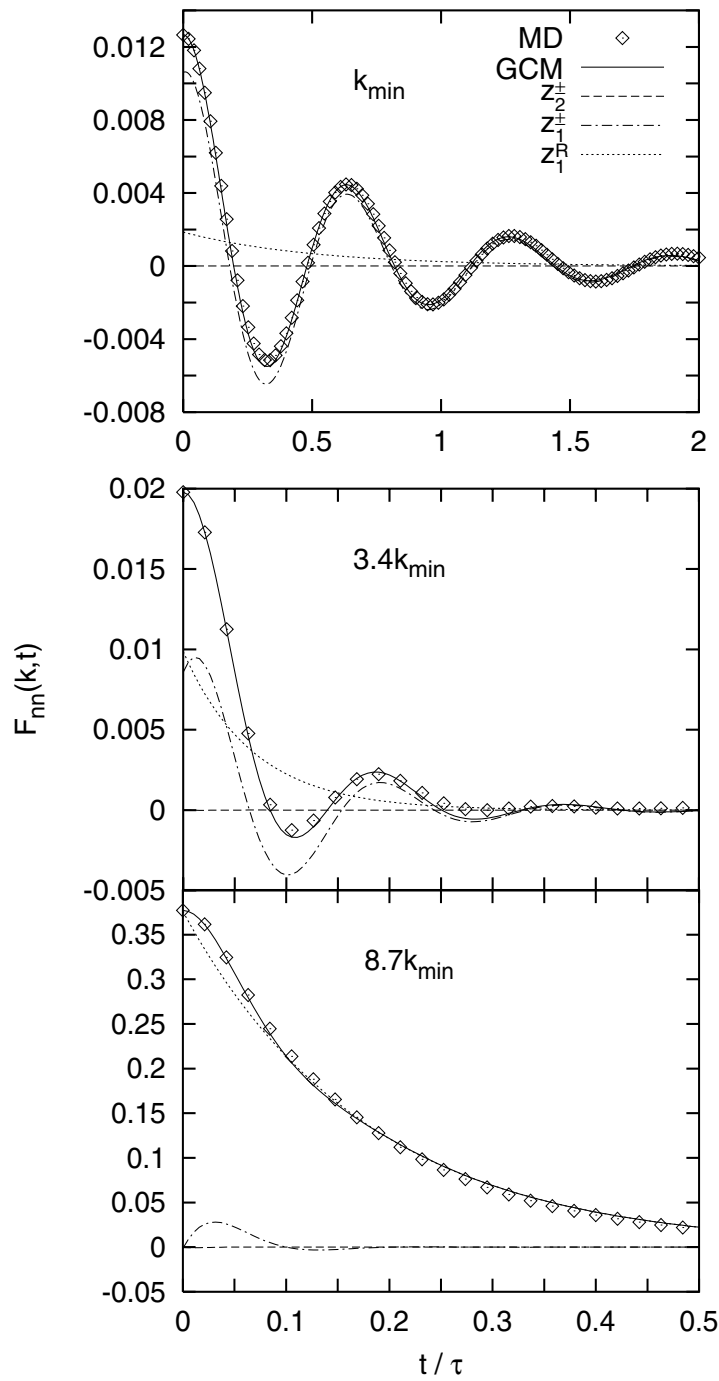


Figure 8. Separated mode contributions to the density–density time correlation functions $F_{nm}(k, t)$ for three k -values. The MD-derived function and the result from GCM study (10) are shown by symbols and solid lines, respectively. Mode contributions from kinetic heat waves, generalized sound excitations, and generalized thermodiffusive modes are given by dashed, dashed–dotted, and dotted lines, respectively. k_{\min} and τ are 0.1928 \AA^{-1} and 3.42 ps , respectively.

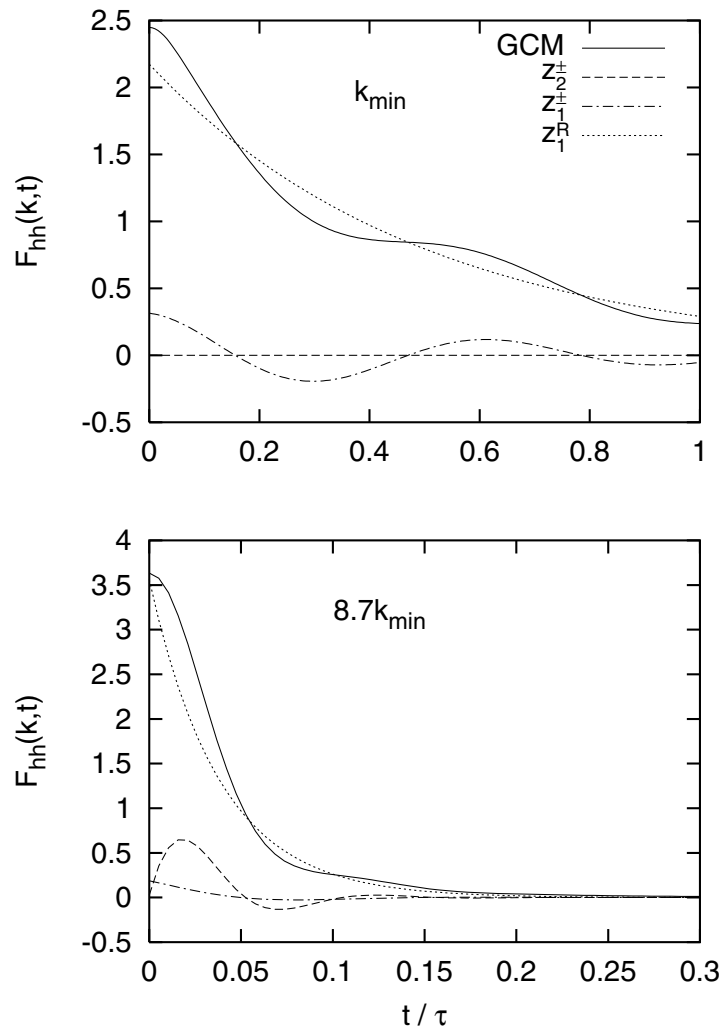


Figure 9. Separated mode contributions to the heat-density–heat-density time correlation functions $F_{hh}(k, t)$ for two k -values. Reduced units are used. All of the other features are the same as in figure 8.

sound modes are reduced and the contributions of heat waves become even stronger than those of sound excitations. In figure 9 one can see that for large k -values the heat waves substantially contribute to the time correlation function $F_{hh}(k, t)$.

4. Conclusions

The main results of this study are the following:

- (i) The spectrum of collective excitations of liquid-semimetallic Bi obtained within the high-number-of-variables approximation of the parameter-free method of generalized collective modes contains three branches of propagating excitations: generalized sound modes and two *high-frequency kinetic* branches.

- (ii) Heat fluctuations cause not only thermodiffusive processes in liquid-semimetal Bi, but also kinetic high-frequency heat waves, with sound-like dispersion, which at $k \rightarrow 0$, however, tends to a finite value.
- (iii) In the case of Bi, the high-frequency heat waves have extremely small weights to make visible contributions to the density–density time correlation functions. This means that high-frequency kinetic excitations in the case of liquid Bi cannot have an effect on the dynamic structure factor, which is supposed to occur in the case of another semimetal, Ga [3]. The mode-coupling effects in liquid Bi at 578 K are found to be very small. This results in very good agreement of the speed of sound estimated in this study with its experimental value.
- (iv) To our knowledge, this study is one of the first investigations of heat waves in a pure liquid from the microscopic point of view in contrast to the phenomenological approach used in the frameworks of physics of continuous media [35].

Acknowledgments

This work was supported in part by the Welch Foundation (Houston, Texas) and the National Academy of Sciences of Ukraine. IM is grateful for the support of the Fonds für Förderung der wissenschaftlichen Forschung under Project P12422 TPH.

References

- [1] March N H 1990 *Liquid Metals. Concepts and Theory* (Cambridge: Cambridge University Press)
- [2] Dzugutov M and Dahlborg U 1989 *Phys. Rev. A* **40** 4103
- [3] Bermejo F J, Fernandez-Perea R, Alvarez M, Roessli B, Fischer H E and Bossy J 1997 *Phys. Rev. E* **56** 3358
- [4] Bosse J, Jacucci G, Ronchetti M and Schirmacher W 1986 *Phys. Rev. Lett.* **57** 3277
- [5] Campa A and Cohen E G D 1988 *Phys. Rev. Lett.* **61** 853
- [6] Alvarez M, Bermejo F J, Verkerk P and Roessli B 1998 *Phys. Rev. Lett.* **80** 2141
- [7] Parrinello M and Tosi M P 1979 *Rev. Nuovo Cimento* **2** No 6
- [8] March N H and Parrinello M 1982 *Collective Effects in Solids and Liquids* (Bristol: Hilger)
- [9] Bryk T and Mryglod I 1999 *Phys. Lett. A* **261** 349
- [10] Morkel Chr, Bodensteiner T and Gemperlein H 1993 *Phys. Rev. E* **47** 2575
- [11] Boon J-P and Yip S 1980 *Molecular Hydrodynamics* (New-York: McGraw-Hill)
- [12] Hansen J-P and McDonald I R 1986 *Theory of Simple Liquids* (London: Academic)
- [13] de Schepper I M, Cohen E G D, Bruin C, van Rijs J C, Montfrooij W and de Graaf L A 1988 *Phys. Rev. A* **38** 271
- [14] Mryglod I M, Omelyan I P and Tokarchuk M V 1995 *Mol. Phys.* **84** 235
- [15] Mryglod I M and Omelyan I P 1995 *Phys. Lett. A* **205** 401
- [16] Bryk T and Chushak Y 1997 *J. Phys.: Condens. Matter* **9** 3329
- [17] Bryk T and Mryglod I 1998 *J. Phys. Stud. (Ukraine)* **2** 322
- [18] Bertolini D and Tani A 1995 *Phys. Rev. E* **51** 1091
- [19] Westerhuijs P, Montfrooij W, de Graaf L A and de Schepper I M 1992 *Phys. Rev. A* **45** 3749
- [20] Bryk T, Mryglod I and Kahl G 1997 *Phys. Rev. E* **56** 2903
- [21] Bryk T and Mryglod I 1999 *Condens. Matter Phys. (Ukraine)* **2** 285
- [22] Mryglod I 1998 *Ukr. Phys. J.* **43** 252
- [23] Bryk T and Mryglod I 2000 *J. Phys.: Condens. Matter* submitted
- [24] Dzugutov M 1989 *Static and Dynamic Properties of Liquids* ed M Davidovic and A K Soper (Berlin: Springer)
- [25] Bryk T and Mryglod I 2000 *Phys. Rev. E* to be submitted
- [26] de Schepper I M, Verkerk P, van Well A A and de Graaf L A 1984 *Phys. Lett. A* **104** 29
- [27] Morozov V G 1983 *Physica A* **117** 511
- [28] Mryglod I 1999 *J. Phys. Stud. (Ukraine)* **3** 33
- [29] Blairs S and Joasoo U 1980 *J. Inorg. Nucl. Chem.* **42** 1555
- [30] Inui M, Takeda S and Uechi T 1992 *J. Phys. Soc. Japan* **61** 3203
- [31] Götze W and Lücke M 1975 *Phys. Rev. A* **11** 2173

- [32] Bosse J, Götze W and Lücke M 1978 *Phys. Rev. A* **17** 434
- [33] March N H and Tosi M P 1976 *Atomic Dynamics in Liquids* (London: Macmillan)
- [34] Balucani U and Zoppi M 1994 *Dynamics of the Liquid State* (Oxford: Clarendon)
- [35] Joseph D D and Preziosi L 1989 *Rev. Mod. Phys.* **61** 41